Table of Contents

Numerical Simulation of Ventilation Efficiency in Commercial Kitchen

Yasushi Kondo[1], Shin-ichi Akabayashi[2], Osamu Nagase[3] and Akihiko Matsuda[4]

[1] Dept. of Architecture, Musashi Institute of Technology, Tokyo, Japan
[2] Dept. of Architecture, Niigata Univ., Niigata, Japan.
[3] Mechanical & Electrical Engineering Dept., Nikken Sekkei Ltd. , Tokyo, Japan
[4] Air-conditioning & Commercial Sales Dept., Tokyo Gas Co. Ltd. , Tokyo, Japan

ABSTRACT

In this paper, the airflow and temperature distributions in a commercial kitchen are simulated based on the k-ε model, and the ventilation efficiency is investigated for three types of ventilation systems. The result of this simulation shows that the suitable supply method of the outdoor air and the conditioned air can give high ventilation efficiency, and thus the kitchen can be kept comfortable with relatively low energy consumption.

KEYWORDS

Kitchen ventilation, CFD and Ventilation efficiency.

INTRODUCTION

It is well known that the amount of energy consumption for ventilation and air-conditioning in the kitchen is much larger than in the other kinds of rooms. In the commercial kitchen, a huge ventilation rate is necessary to remove the exhausted gas from the cooking gas range and the other devices. Therefore the large energy is consumed when the outdoor air supplied into the room is conditioned in order to keep the working area at a moderate temperature. On the other hand, if the outdoor air is not conditioned, it is difficult to keep the room comfortable.

This paper is concerned with the ventilation system in which the fresh

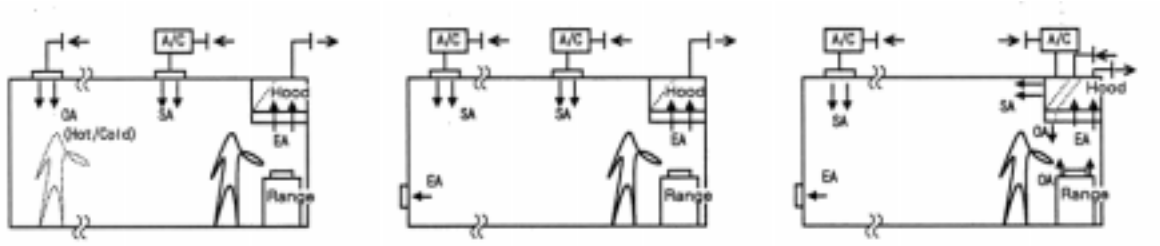

(a) Local Air-conditioning (Outdoor air for ventilation is not conditioned.) (Energy consumption is small, but it is not comfortable.)

(b) Entire Air-conditioning (Outdoor air for ventilation is conditioned.) (It is comfortable, but Energy consumption is large.)

(c) System Investigated in This Paper

Figure 1 Ventilation and Air-conditioning System in Commercial Kitchens

(1) Improvement of Ventilation Efficiency : Outdoor air is supplied near the cooking range in order to be induced to the updraft above the range.
(2) Improvement of Air-conditioning Efficiency : The working area is expected to be kept at moderate temperature by minimizing the influence of the high temperature region near the range.

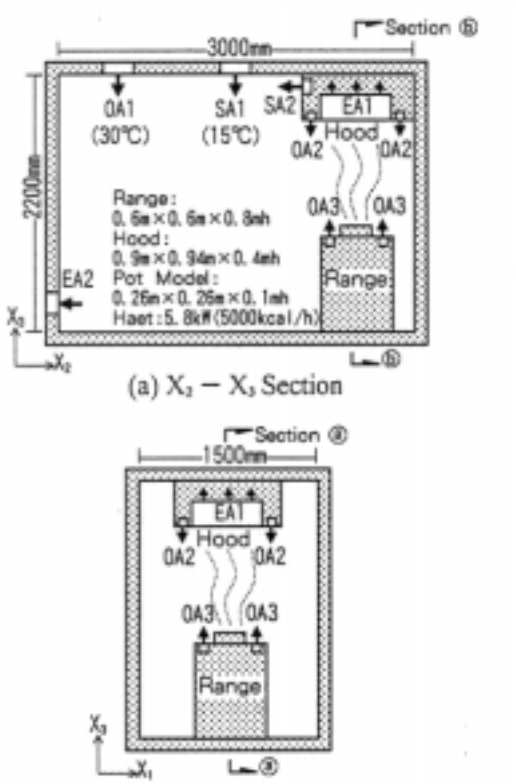

Figure 2 Kitchen Model for Simulation

OA : Outdoor Air for Ventilation
SA : Supplied Air for Air-conditioning
EA : Exhausted Air

air is supplied near the cooking range as shown in Figure 1. In this system, it is expected to that the heat and the gas exhausted from the range can be removed efficiently by arranging the suitable velocity and the direction of fresh air outlets. The air-conditioning is also effective in the occupied zone because the air-conditioning efficiency can be improved by minimizing the influences of the hot (or cold) outdoor air and the hot and humid air from the range.

In order to evaluate the effectiveness of the ventilation and the air-conditioning in the kitchen, the numerical simulation is conducted based on the k-ε model. The temperature of air and obstacle surfaces (e.g. wall) and the air velocity

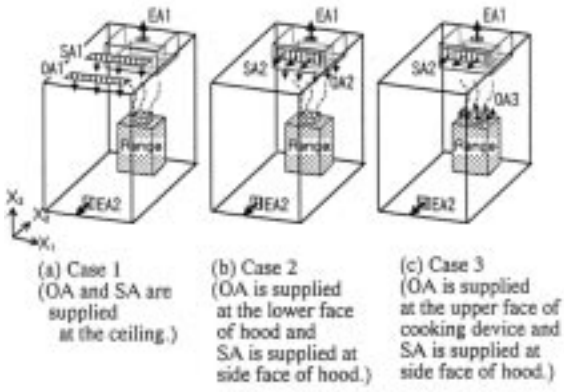

Figure 3 Outline of Simulated Cases

Table 1 Condition of Ventilation and Air-conditioning

	Case 1	Case 2	Case 3
Air-conditioning	SA1	SA2	SA2
	400m³/h 15°C 0.427m/s 0.26m×1m	400m³/h 15°C 0.871m/s 0.15m×0.85 m	400m³/h 15°C 0.871m/s 0.15×0.85m
Ventilation	OA1	OA2	OA3
	400m³/h 30°C 0.427m/s 0.26×1m	400m³/h 30°C 0.463m/s 0.1m×0.6m×4	400m³/h 30°C 0.794m/s 0.1m×0.35m×4
Exhaust	EA 1(Hood)	EA 1(Hood)	EA 1(Hood)
	400m³/h 0.6m×0.6m	400m³/h 0.6m×0.6m	400m³/h 0.6m×0.6m
	EA2	EA2	EA2
	400m³/h 0.2m×0.2m	400m³/h 0.2m×0.2m	400m³/h 0.2m×0.2m

are obtained from the interactive simulation of the radiative heat transfer and the convective one. The numerical results are compared with the model experiments (Akabayashi et al., 1998) and the correspondence between them is examined.

Furthermore, the SVEs (Scale for Ventilation Efficiency, Murakami and Kato 1992) is used to investigate the influence of the fresh air and how the exhausted gas from the range is captured in the kitchen hood.

1 METHOD OF NUMERICAL STUDY

1.1 Model of Kitchen

The modeled kitchen with the same scale of the experiment chamber (a depth of 3.0m, a width of 1.5m and a height of 2.2m, Akabayashi et al. 1998) is simulated as shown in Figure 2. The model is supposed to be a part of a large commercial kitchen and the amount of heat from the cooking range is assumed to be 5.8kW(5000kcal/h). The numerical simulations are conducted for the kitchen space under the cooling condition in which 400m^3/h of conditioned air at 15°C and the same volume of outdoor air at 30 °C are supplied as described in Table 1.

1.2 Cases Calculated

Figure 3 shows three types of ventilation systems treated in this simulation. In Case 1, both the conditioned air (15°C) and the outdoor air (30°C) are supplied from the ceiling downward. In Case 2, the outdoor air is supplied from the lower faces of the hood downward and the conditioned air is supplied from the side face of the hood horizontally. In Case 3, the outdoor air is supplied at the upper faces of the cooking equipment upward and the conditioned air is supplied in the same way as in Case 2. Case 2 and Case 3 are expected to be ventilation systems with high ventilation efficiency and they are compared with Case 1 that is assumed to be a general kitchen ventilation system.

Table 2 Boundary Condition for Numerical Simulation

Supply Opening	Velocity (Uin) and temperature (Θin) are given as shown in Table 1. Turbulent kinetic energy (k) is set to be (Uin / 10)^2. Turbulent length scale is set to be a half of opening length.
Exhaust Opening	Velocity (Uout) is given as shown in Table 1. Turbulent kinetic energy, dissipation ratio (**ε**), and temperature are set to be satisfied the free slip condition.
Wall Surface	Velocity is solved by the generalized log-law type wall function. Temperature is obtained by solving the balance equation which includes conduction, convection and radiation as below; Qcd+Qcv+Qr=0 at wall surface. 1 Heat conduction (Qcd) is given to be 5.8kW (5000kcal/h) at the pot model surface and to be 0 kW (adiabatic) at other walls. 2 Convective heat flux (Qcv) is calculated by αc type wall function ; Qcv=αc×(Θw-Θ1). WhereΘw is wall surface temperature and Θ1 is air temperature of the first mesh in CFD. The value of αc is given to be 16 kcal/m^2 h °C at the pot model and to be 8 kcal/m^2 h °C at other walls. 3 Radiative heat flux (Qr) is evaluated as ; $Qr=Tm^3 \sigma \varepsilon i \sum Bij(\Theta wi-\Theta wj)$ Where Tm is mean temperature (=300K), Bij is Gebhart's absorption factor, σ is Stefan-Boltsman constant andεi is emissivity of i-th wall.

Table 3 Simulation Condition

Spatial coordinate (X_1, X_2, X_3) is illustrated in Figure 2 and 3. Kitchen model is divided into 18 (X_1) ×57 (X.) ×37 (X.) =37,962 meshes. QUICK scheme is used in calculating the convective term of momentum equation in CFD. Only a half of entire space is simulated with aid of symmetry of model in X_2 direction. Shape factor required for radiative heat transfer simulation is calculated for boundary elements of model surface. The number of surface boundary elements is 93 in total and 100,000 radiative ray are emitted from each element in Monte-Carlo method.

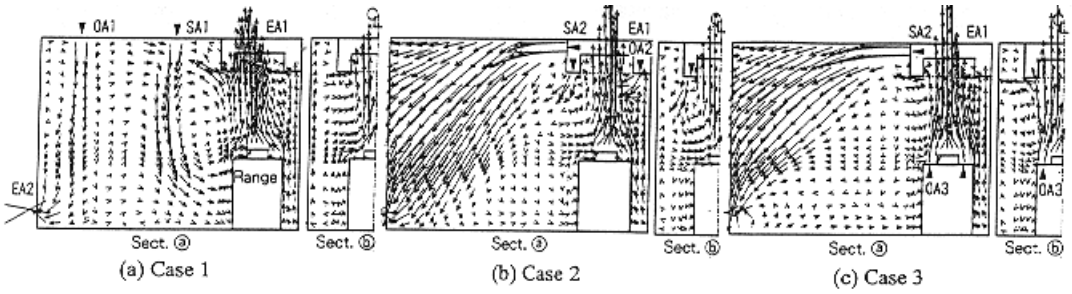

Figure 4 Airflow Distribution

*Sect. ⓐ and Sect. ⓑ are shown in Figure 2.

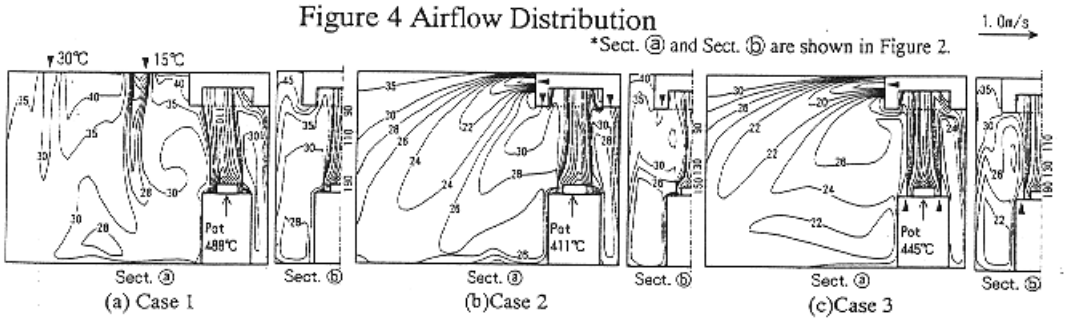

Figure 5 Air Temperature Distribution (℃)

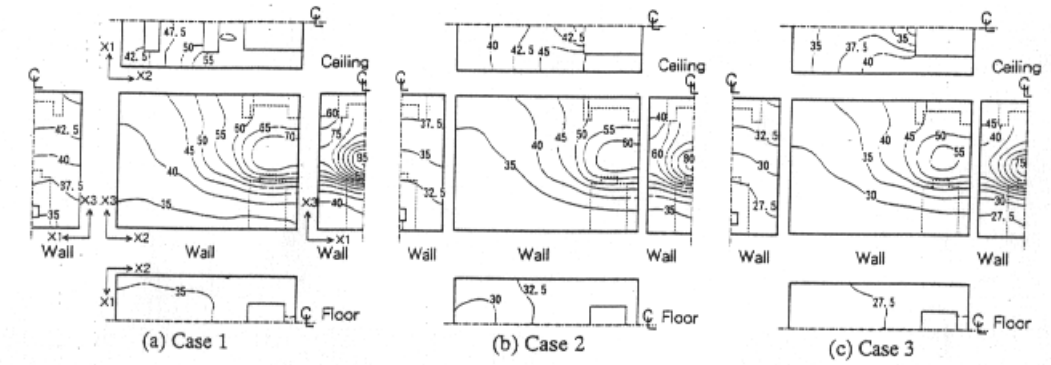

Figure 6 Distribution of Wall Surface Temperature (℃)

1.3 Simulation Method

An airflow analysis was carried out based on the standard k-ε turbulence model with a wall function type boundary condition. The surface temperature of an object such as walls was obtained by solving the heat balance equation in which the convective and radiative heat transfer were combined. The shape factor which is necessary for the radiative heat transfer simulation was calculated by the Monte-Carlo method prior to the CFD. The boundary condition and the other conditions for numerical simulation are shown in Table 2 and Table 3 respectively.

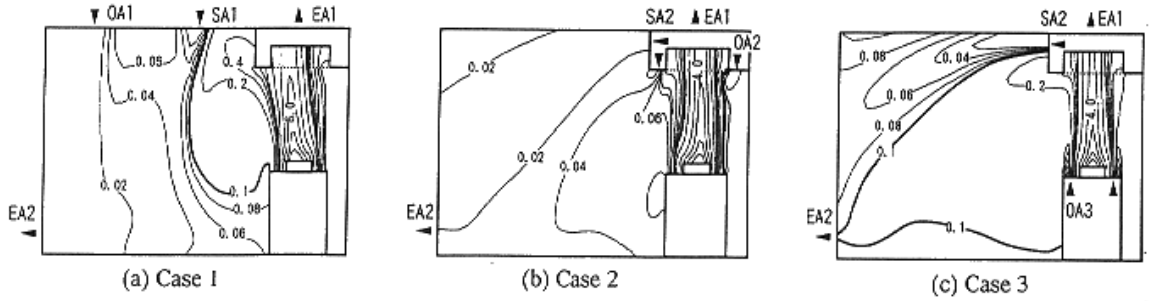

(a) Case 1 (b) Case 2 (c) Case 3

Figure 7 Distribution of Passive Contaminant Generated at Cooking Range

2 RESULTS OF NUMERICAL SIMULATION

2.1 Airflow Distribution

Figure 4 compares the airflow distribution of three cases. The thermal plume caused by the heat from the cooking range is observed and this updraft is captured into the hood in Case 2 and Case 3. However, in Case 1 one part of the updraft flows out of the hood. The jet supplied from the hood horizontally descends by the buoyancy effect due to the temperature difference between the jet air and the surrounding air in Case 2 and Case 3. This temperature difference in Case 2 is larger than in Case 3 as will be described later, therefore the horizontal jet of Case 2 goes down slightly stronger than that of Case 3.

2.2 Air Temperature Distribution

Figure 5 shows the distribution of air temperature in which the working area is very hot in Case 1; on the other hand it is rather comfortable in Case 2 and Case 3. This is because that the ventilation and air-conditioning efficiency in Case 2 and Case 3 is much better than that in Case 1. This ventilation efficiency can be explained from the contribution ratio of the hot outdoor air in the working space as will be mentioned later. In Case 1, the hot outdoor air has a larger power in the working space than in other cases, the air temperature thus increases due to the hot outdoor air.

2.3 Wall Surface Temperature

Figure 6 shows the temperature distribution of the wall surface. The wall surface temperature is strongly influenced by the radiation from the pot model set on the cooking range in all cases. The wall temperature in Case 1 is higher than in other cases according with the difference of air temperature mentioned above.

3 VENTILATION EFFICIENCY

The ventilation efficiency of each case is evaluated by SVEs (Scale for Ventilation Efficiency) proposed by Murakami and Kato (1992) in order to confirm the characteristics of each ventilation system. Table 4 shows the calculation method of SVEs.

3.1 Distribution of Contaminant/Heat Generated at Cooking Range

The transport equation of the passive scalar contaminant is solved in which it is supposed to be generated at the surface of the pot model on the cooking range. Figure 7 compares the passive scalar distribution of each case. In Case 1, the contamination leaked out of the hood is rather large but the area of high concentration such as 0.1 of the normalized concentration line is not so large, because the supplied air at the

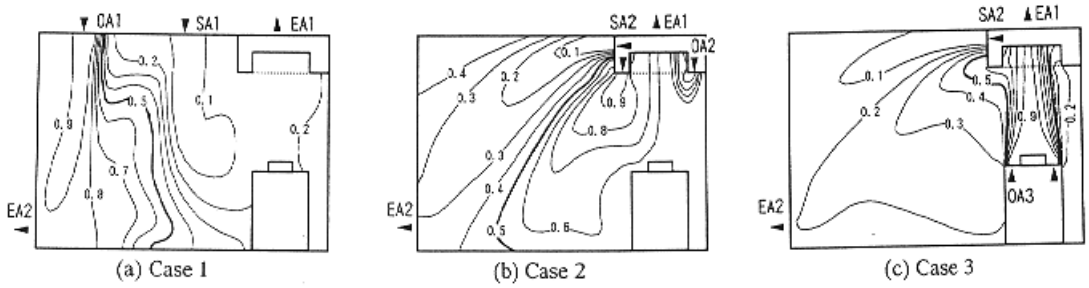

(a) Case 1 (b) Case 2 (c) Case 3

Figure 8 Contribution Ratio of Supplied Outdoor Air

Table 4 Calculation Method of SVEs

etc.
1 Distribution of contaminant/heat generated at cooking range : It is supposed that passive contaminant is generated at the pot model surface. Transport equation of contaminant is solved by using the CFD result and the generation rate of contaminant is set to be same as the rate in which the concentration is 1.0 in the perfect mixing condition.
2 SVE4, contribution ratio of supply outlet of hot outdoor air : The passive scalar distribution is calculated under the condition in which the non-dimensional concentrations of outdoor and conditioned air are supposed to be 1.0 and 0.0 respectively.
3 SVE5, contribution ratio of exhaust inlet : The passive scalar distribution is calculated under the condition in which the airflow direction obtained by CFD is reversed and the non-dimensional concentration is set to be 1.0 at the exhaust hood.

Table 5 Exhausted Rates of Scalar Generated at Pot Model and Outdoor Air through the Hood Opening

	Case 1		Case 2		Case 2	
	Sim.	Exp.	Sim.	Exp.	Sim.	Exp.
Exhausted rate of scalar generated at pot	98%	95%	99%	81%	95%	76%
Exhausted rate of outdoor air	14%	38%	63%	63%	79%	61%

- Exhausted rate of the simulation shown above is obtained by summing up the passive scalar concentration at the hood opening.
- Exhausted rate of the experiment shown above means the capture rate of combustion gas from cooking range and tracer gas injected in the outdoor (see Akabayashi et al. 1998).

ceiling restrains the diffusion of the leaked air from the hood. On the other hand, the result of Case 3 shows that the ratio of leaked air is smaller than that in other case but the high concentrated area is rather wide. The calculated amounts of the captured scalar at the hood are shown in Table 5 with the experimental results.

3.2 Contribution Ratio of Supply Opening (SVE 4)

The results of concentration for each case are shown in Figure 8 when non-dimensional concentration is set to be 1.0 at the supply point of outdoor air. This index is SVE4 proposed by Murakami and Kato (1992) in order to estimate the power of supplied air in the space. This paper focuses on the SVE4 of the hot outdoor air. The SVE4 of Case 1 is much larger in the working area than that of other cases, therefore the air temperature is high due to the influence of hot outdoor air

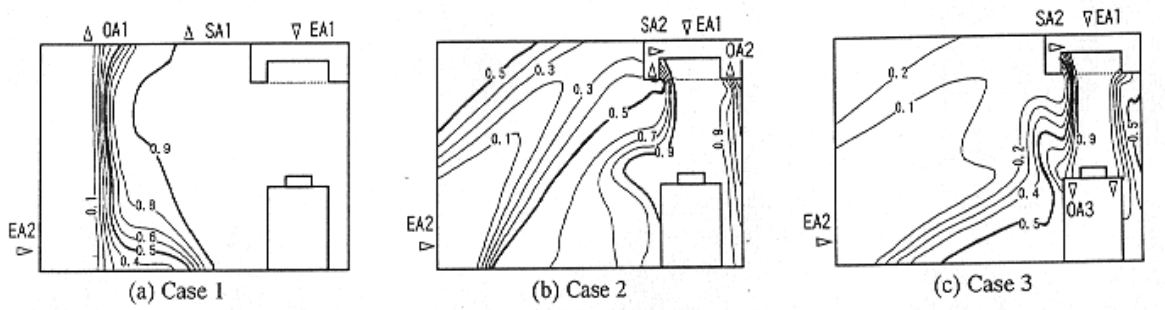

(a) Case 1 (b) Case 2 (c) Case 3

Figure 9 Contribution Ratio of Exhaust Hood

(30°C) in such regions. In Case 2, the outdoor air is very powerful near the cooking range. The area of high SVE4 value is the smallest in Case 3 which has a high ventilation efficiency with a suitable supply position of hot outdoor air. The total amounts of SVE4 at the exhaust hood are shown in Table 5 (see Note 1). The 14% of the outdoor air volume is exhausted from the hood in Case 1, but more than 60% of outdoor air is captured by the hood in Case 2 and Case 3. The contribution ratio of the conditioned air (15°C) can be evaluated by subtracting the SVE4 value of outdoor air from 1.0 in this situation. The power of conditioned air is dominant in the working area in Case 3, therefore the air temperature can be kept in a more comfortable range than in other cases, meaning that the air-conditioning efficiency is excellent in Case 3.

3.3 Contribution Ratio of Exhaust Hood (SVE5)

In order to estimate the power of the exhaust hood, the passive scalar distribution is calculated under the condition in which the airflow direction obtained by CFD is reversed and the non-dimensional concentration is set to be 1.0 at the point of the exhaust hood. The results of concentration for each case are shown in Figure 9. This index is SVE5 proposed by Murakami and Kato (1992) in order to estimate the contribution ratio of the exhaust inlet. In Case 1, the region of high SVE5 value is extended to the working area. On the other hand, the dominant area of the hood in Case 3 is much smaller than that in other cases, which means that the local exhaust is achieved efficiently in Case 3.

CONCLUSION

In this paper, the airflow and thermal fields are simulated for the modeled kitchen under the cooling condition. The ventilation and air-conditioning efficiency is studied for the three types of ventilation systems by SVEs. The obtained results are as follows.

(1) When the hot outdoor air (30°C) is supplied at the position near the cooking range such as the lower faces of the hood or the upper faces of the cooking equipment, the power of the outdoor air (SVE4) is not strong in the working space. In these cases, it is possible to maintain a comfortable environment in the working area.

(2) In Case 3 with the outdoor air supply outlet at the upper faces of the cooking equipment, the power of the exhaust hood (SVE5) is limited near the cooking range and the local ventilation is effective.

REFERENCES

S. Akabayashi, Y. Kondo, J. Sakaguchi and T. Kawase : Experimental Study on Ventilation Efficiency in Commercial Kitchens, ROOMVENT '98 submitted.

S. Kato and S. Murakami : New Scales for Evaluating Ventilation Efficiency as Affected by Supply and Exhaust Openings Based on Spatial Distribution of Contaminant, International Symposium on Room Air Convection and Ventilation Effectiveness(ISRACVE), 1992.7, pp321-332.

Y. Kondo, S. Akabayashi, T. Kawase, K. Ogata and T. Yoshioka : Study on Air-conditioning and Ventilation System of Kitchen, Part 4 Numerical Simulation of Flow and Temperature Distributions and Ventilation Efficiency, Annual meeting, SHASEJ, 1994.10, pp201-204. (In Japanese)

Note 1: There exist the compression of air due to high temperature and the huge moisture generation near the cooking gas range, so that the air and heat diffusion is very active in such region. However, these effects are not included in the numerical. Therefore the diffusion of the simulated plume over the gas range may be under-estimated, and the simulated temperature of updraft is much higher than the experimental result as shown in Figure 10. This difference also appears in the capture ratio of the combustion gas and the heat from the cooking range as shown in Table 5.

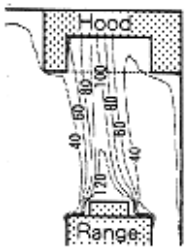

(a)Result of Simulation : Case 1

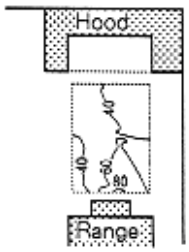

(b)Result of Experiment (Akabayashi et al. 1998)

Figure 10 Thermal Plume above the Cooking Range